ORIGINAL RESEARCH

Gentiopicroside-Loaded Chitosan Nanoparticles Inhibit TNF-α-Induced Proliferation and Inflammatory Response in HaCaT Keratinocytes and Ameliorate Imiquimod-Induced Dermatitis Lesions in Mice

Kaixuan Zhao[1],*, Siqi Pu ⓘ[2],*, Liyun Sun[1], Dongmei Zhou[1]

[1]Dermatology Department, Beijing Hospital of Traditional Chinese Medicine, Capital Medical University, Beijing, 10010, People's Republic of China; [2]School of Clinical Medicine, Beijing University of Chinese Medicine, Beijing, People's Republic of China

*These authors contributed equally to this work

Correspondence: Liyun Sun, Dermatology Department, Beijing Hospital of Traditional Chinese Medicine, Capital Medical University, 23 Art Musuem Back Street, Dongcheng District, Beijing, 100010, People's Republic of China, Email doctorsunny@sina.cn; Dongmei Zhou, Dermatology Department, Beijing Hospital of Traditional Chinese Medicine, Capital Medical University, 23 Art musuem Back street, Dongcheng District, Beijing, 100010, People's Republic of China, Email 52176857@163.com

Purpose: In this study, we aimed to report the biological characteristics of the first successful synthesis of gentiopicroside-loaded chitosan nanoparticles and to evaluate the therapeutic effects and preliminary mechanisms of gentiopicrin-loaded chitosan on psoriasis-like cell and mouse models.

Methods: Gentiopicroside-loaded chitosan nanoparticles (CHI-GEN) were prepared, and their biological characteristics were evaluated. HaCaT keratinocytes were stimulated with TNF-α to establish a psoriatic keratinocyte model. MTT assay and flow cytometry were used to measure cell viability and apoptosis, respectively. mRNA levels of K17, VEGF A, and IL-6 and IL-23A were detected using qRT-PCR. These tests were used to preliminarily assess the effects of CHI-GEN on keratinocyte proliferation and inflammation. Imiquimod was used to construct a psoriasis-like mice model. The severity of psoriasis was scored based on the psoriasis area severity index (PASI), H&E staining was used to observe the histological changes and the level of inflammation and cell proliferation of skin lesions was evaluated by measuring the mRNA levels of K17, IL-23A, and IL-17A using qRT-PCR.

Results: The average particle size of CHI-GEN nanoparticles was approximately 100 nm, and the zeta potential was 2.69 ± 0.87 mV. The cumulative release was 67.2% in solutions of pH 5.5 at 24 h. GEN reduced TNF-α-induced excessive proliferation of HaCaT keratinocytes and downregulated mRNA levels of K17, VEGF A, and inflammatory cytokines IL-6 and IL-23A, which was more obvious in the CHI-GEN treatment group. Additionally, CHI-GEN significantly improved the severity of skin lesions in psoriasis-like mice and downregulated the mRNA expressions of IL-6, IL-23A, and IL-17A in mice skin lesions.

Conclusion: In conclusion, we successfully prepared gentiopicrin-chitosan nanoparticles. Our results show that these nanoparticles have anti-psoriasis activity, inhibits keratinocyte proliferation and improves symptoms in psoriasis model mice and can be used to develop an effective strategy for the treatment of psoriasis.

Keywords: chitosan, nanoparticles, gentiopicroside, chitosan-loaded nano cream for external use, psoriasis, proliferation and inflammation

Introduction

Psoriasis is a chronic inflammatory skin disease characterized by erythema, scaling, and thickness. It is characterized by excessive proliferation and abnormal differentiation of epidermal keratinocytes, as well as increased infiltration of immune

cells and intracutaneous angiogenesis.[1,2] The disease course is long and prone to relapse which seriously affects the physical and mental health of patients. Psoriasis may also induce various complications, such as psoriatic arthritis, metabolic syndrome, non-melanoma skin cancer, and cardiovascular diseases.[3] In recent years, the incidence of this disease is on the rise, ranging from 0.09% to 11.43% in different countries. About 125 million people suffer from this disease worldwide, bringing a serious economic burden to society and the families of patients.[4]

Psoriasis is a multigenic and environmentally induced autoimmune disease, whose pathogenesis is complex and has not been fully elucidated.[1] Keratinocytes and infiltrating immune cells play a key role in the pathogenesis and development of psoriasis.[5] In psoriatic lesions, immune cells secrete various cytokines to stimulate keratinocytes leading to their excessive proliferation, which in turn responds to these cytokines by producing many pro-inflammatory cytokines to maintain and amplify the inflammatory response.[6–8] Therefore, drugs that inhibit keratinocyte overproliferation and inflammation have the potential for the treatment of psoriasis.

Although biologics such as methotrexate, cyclosporine, UVB irradiation, and topical drugs have achieved certain clinical efficacy, psoriasis cannot be completely cured and has a high recurrence rate. Additionally, long-term use of the available treatment regimens has considerable side effects.[9–11] Therefore, it is necessary to develop new and effective anti-psoriasis drugs with fewer side effects. Over the years, traditional medicine has had curative effects in the treatment of psoriasis. An in-depth study of traditional medicine using modern pharmacological and chemical methods revealed that natural products such as amygdalin analog,[12] rosmarinic acid,[13] and resveratrol,[14] extracted in the form of chemical monomers or other chemical forms, can treat psoriasis by inhibiting keratinocyte proliferation.[15]

Gentiopicroside is an iridoid glycoside primarily extracted from *Gentiana macrophylla*[16–18] and has anti-inflammatory, antioxidant, analgesic, and other pharmacological effects.[19–23] Gentiana, a member of the Genus *Gentiana*, is a traditional Chinese medicine used in the treatment of psoriasis. Our preliminary study found that a Chinese herbal compound containing *Gentiana macrophylla* showed clinical efficacy in the treatment of psoriasis. Gentiopicroside is a water-soluble molecule with a low oil-water distribution coefficient, strong hydrophilicity, and poor lipid solubility. Therefore, it cannot penetrate the lipid skin solubility barrier and has weak permeability for external application, which limits the development and application of Gentiopicroside in the treatment of psoriasis.

Chitosan is a cationic marine natural polysaccharide obtained from chitin after N-acetylglucosamine deacetylation,[24,25] which is a partial deacetylation derivative obtained after the alkaline treatment of chitin. Compared with traditional pharmaceutical excipients, chitosan nanoparticles have many favorable biological characteristics including biodegradability, low cytotoxicity, high bioavailability, and excellent biocompatibility and hence, can be used as carriers for drug delivery.[26,27] Several studies have shown that topical and external drug-loaded chitosan nanoparticles have achieved promising effects in the treatment of psoriasis,[28–30] diabetic skin injury,[31] chloasma,[32] viral skin infections,[33] and other skin diseases.

Based on the biological characteristics of chitosan such as high bioavailability and biocompatibility, this study aims to make gentiopicroside play a better role in the treatment of psoriasis through topical application. In this study, to the best of our knowledge, we prepared for the first time, gentiopicroside-loaded chitosan nanoparticles, and evaluated in vitro the effects of CHI-GEN nanoparticles on proliferation, apoptosis, and cytokine expression of HaCaT cells induced by tumor necrosis factor α (TNF-α). We further tested the anti-psoriasis efficacy of gentiopicroside-loaded chitosan nanocream in imiquimod (IMQ)-induced psoriatic dermatitis in BALB/c mice and determined its therapeutic effect on psoriasis.

Materials and Methods
Chemicals and Reagents

Gentiopicroside was purchased from Beijing Zhongke Quality Inspection Biotechnology Co., Ltd. (Beijing, China). Chitosan was purchased from Sinopharm Chemical Reagent Co., Ltd (Shanghai, China). Aldara IMQ Cream was obtained from 3M Health Care Limited (Shanghai, China). TNF-α cytokines were purchased from PeproTech (Cranbury, NJ, USA). BALB/c mice were purchased from Beijing Weitong Lihua Laboratory Animal Co., Ltd. (Beijing, China). HaCaT cells were purchased from Cell Resource Center, Institute of Basic Medical Sciences, Chinese Academy of Medical Sciences (Beijing, China).

Minimum essential medium (MEM) and fetal bovine serum (FBS) were purchased from Gibco (Waltham, MA, USA). Penicillin-streptomycin mixture, annexin V-FITC/PI apoptosis detection kit, and trypsin-EDTA solution (TRY) were obtained from Solarbio Life Science (Beijing, China). MTT (3-(4,5-Dimethylthiazol-2-yl)-2,5-diphenyltetrazolium bromide) was purchased from Beijing Aokesi Technology Co., Ltd. (Beijing, China) and methotrexate (MTX) was purchased from Shanghai Yuanye Biotechnology Co., Ltd (Shanghai, China). ReverTra Ace®qPCR RT master mix with gDNA remover kit and SYBR®qPCR mix kit were purchased from TOYOBO (Tokyo, Japan).

Preparation and Characterization of Gentiopicroside-Loaded Chitosan Nanoparticles
Preparation
The self-assembled hydroxyethyl chitosan, which is a carrier for the delivery of gentiopicroside, was prepared as previously described by Han et al.[34] Gentiopicroside solution was prepared by mixing gentiopicroside (4 mg) and PBS (10 mL) and then dropping it into anhydrous ethanol (20 mL) containing dissolved hydroxyethyl chitosan nanoparticles (10 mg). The mixture was stirred for 2h and ethanol was removed to obtain a gentiopicroside-loaded chitosan nanoparticle solution.

Characterization Using Transmission Electron Microscopy (TEM)
CHI-GEN and CHI solutions were dropped on the copper mesh (400 mesh) for air drying, then 1% tungsten phosphate aqueous solution was dropped on the glass sheet. The copper retina side, containing the sample, was inverted on the tungsten phosphate water drop, left undisturbed for 2 min, and then inverted on the clean water drop for washing for approximately 30s following which the sample was air-dried. The chemical structure and functional groups of blank CHI and CHI-GEN nanoparticles were analyzed using TEM (JEOL, 1011). The operating voltage was 100 kV.

Measurement of Dynamic Light Scattering and Zeta Potential
The mean hydrate particle size and surface charge (zeta potential) of CHI-GEN nanoparticles were evaluated using the Brookhaven Bi9000AT system (Brookhaven Instruments Corporation, Holtsville, NY, USA) using the dynamic light scattering (DLS) technique.

Test conditions for dynamic light scattering and ZETA potential measurements: incident angle 90°, temperature 25°C, scan time was 3 min and each sample was measured three times.

Absorbance Test
CHI-GEN solution was ultrasonicated for even dispersion. The absorbance of the CHI-GEN solution was measured using ultraviolet-visible spectrophotometer (Hitachi U-2800, Tokyo, Japan) by adding 1000 μL solution to a 1.5 mL colorimetric dish. Water was used as the reference, black lamp was used as the light source, the scanning speed was 200 nm/min, and the scanning wavelength was 190–500 nm.

Evaluation of in vitro Release Kinetics of the Nanoparticles
The prepared CHI-GEN solution was placed in a cellulose membrane dialysis bag with a retained molecular weight of 500kD and dispersed in 250 mL PBS solution of pH 7.4 and pH 5.5 (to simulate human blood and cell lysosomes, respectively) in an oscillating incubator at 37°C and 100 rpm. We collected 1 mL solution and replaced it with fresh PBS at predetermined time intervals. The collected samples were measured using ultraviolet-visible spectrophotometer (Hitachi u-2800) at 270 nm. All measurements were repeated three times.

Evaluation of Cellular Uptake of Nanoparticles
HaCaT cells (5.0×10^5 cells per plate) were cultured in a 35 mm confocal glass plate in a cell incubator at 37°C and 5% CO_2 for 24 h.

Then, the complete medium was replaced with MEM base medium containing FITC-CHI and incubated for 3 h, 6 h, and 12 h, followed by three PBS washes. The cells were incubated with PBS containing Lyso-Tracker (1.0 μM) for 30 min and washed thrice with PBS.

The other dishes were treated with inhibitors (50 μM amiloride, 50 μM chlorpromazine, 10 mM M-β -cyclodextrin) for 0.5 h, and blank control was added to the basal medium. The samples were washed thrice with PBS and FITC-Chi nanoparticles were added and incubated for 12 h. The samples were washed with PBS three times after incubation.

The cell uptake of CHI was visualized using a confocal laser microscope at excitation wavelengths of 488 nm and 594 nm.

Cell Culture and MTT Analysis

TNF-α-induced HaCaT cell proliferation model was used to evaluate the anti-proliferative activity of CHI-GEN. HaCaT cells were inoculated at a density of 1×10^5/mL in a 96-well culture plate. After 24 h, the cells were incubated with different concentrations of GEN, CHI, and CHI-GEN for 24 h. Following this, 100 μL sterile filtered MTT solution (1 mg/mL) was added to each well, and the cells were cultured at 37°C for 4 h. The unreacted dye was removed, 150 μL DMSO was added to each well, and the crystals were fully dissolved by shaking for 10 min. The light absorption value of each well was measured at the wavelength of 570 nm on a microplate reader, the results were recorded, and cell viability was calculated.

Cell Apoptotic Ratio Was Measured Using Flow Cytometry

HaCaT cells with a concentration of 1×10^6 cells/well were inoculated into a six-well plate, and the control, model, MTX (5 mg/L), GEN (200ng/mL), CHI, and CHI-GEN (50 ng/mL) treatment groups were treated accordingly. The cells were collected and washed with cold PBS, centrifuged at $300 \times g$ for 10 min, and the supernatant was discarded. The cells were resuspended in 1 mL 1× binding buffer to reach the final cell density of 1×10^6 cells/mL. Annexin V-FITC (5 μL) was added to each tube, mixed gently at 20 to 25 degrees Celsius in dark, and centrifuged at 2 g for 5 min. The cell pellet was resuspended in 1× binding buffer (300 μL) and PI (5μL) solution was added and mixed gently at room temperature in dark. The samples were incubated for 5 min. Flow cytometry detection was carried out within 1 h.

Preparation of Cream

The composition of gentiopicroside-loaded chitosan cream (6% gentiopicroside) was as follows: oil phase (M82 0.4 g, A165 0.1 g, ORB 0.1 g, avocado oil 1.6 g), water phase (gentiopicroside 1.2 g, amino acid moisturizer 0.2 g, glycerol polyether-26 0.2 g, hydroxyethyl urea 0.2 g, Henson gum 0.02 g, U30 0.06 g, NA-C 5 g, NaOH 0.12 g, preservative 0.15 g, pure water 11.85 g). The mixture was heated in a water bath to 80°C (until it completely melts), the oil-phase liquid was slowly added to the water-phase liquid and a blender was used to continuously stir the solution till the formation of the cream. A heating pad was used to keep the fusion liquid at 60°C during the stirring process. Gentiopicroside was not included in the preparation of the CHI cream (base cream) and chitosan was not used in the preparation of the GEN cream (monomer control cream).

Experimental Animals

Mice were randomly divided into six groups (five mice in each group): blank group (CON), IMQ group (IMQ), IMQ + base cream group (IMQ+CHI), IMQ+ free gentiopicroside (IMQ + GEN), IMQ + gentiopicroside-loaded chitosan nanoparticles group (IMQ + CHI-GEN), IMQ + Tacrolimus group (IMQ + TK). After 3 days of adaptive feeding, approximately 2×2 cm^2 hair on the back of mice was shaved. Except for the blank group, 62.5 mg 5% IMQ cream was applied to the back of mice daily for 7 days, and the same amount of vaseline was applied to the blank group. After 3 h, a topical dose of 50 mg/cm^2 GEN or CHI-GEN or CHI cream or 0.1% tacrolimus cream was administered for 7 days to the different groups.[35] Based on the psoriatic area severity index (PASI) of the objective scoring system, the erythema, scaling, and thickness of the skin on the back of mice were scored by 0–4 points every day: 0, no; 1, mild; 2, moderate; 3, serious; 4, very severe, and then added to obtain the total severity score throughout the treatment. On day 8, the mice were euthanized and skin samples were collected for subsequent experiments.

Quantitative Real-timePCR (qRT-PCR)

Total RNA was extracted from collected HaCaT cells and back skin samples of mice using TRIzol reagent, and the quantity and quality of the RNA were assessed using a NanoDrop2000 instrument. The mRNA levels of K17, IL-6, and IL-23A in HaCaT cells and IL-17A in the back skin of mice were analyzed using qRT-PCR. Total RNA (2 μg) was reverse transcribed into cDNA using SYBR®qPCR mix kit according to the manufacturer's protocol. The total volume of the PCR reaction system was 20 μL. The PCR amplification conditions were as follows: pre-denaturation at 95°C for 3 min, denaturation at 95°C for 15s, denaturation at 60°C for 15 s, and extension at 72°C for 45s, with a total of 40 cycles; dissolution curve: 95°C for 15 s. GAPDH and actin were used as endogenous controls in cells and mice, respectively. StePOnePlus was used for mRNA quantification. PCR primers (Table 1 and Table 2) were synthesized using PCR technology, and the relative expression levels of target genes were determined using the $2^{(-\Delta\Delta CT)}$method.

Animal Ethical Statement

Female (SPF) BALB/c mice (6–8 weeks) with an average body weight of 20 ± 2 g were purchased from Beijing Weitonglihua Laboratory Animal Co., Ltd. (Beijing, China). The mice were kept in constant temperature and humidity with 12 h light/dark cycles and were allowed to freely access food and water. All experimental protocols followed Beijing Ethical review guidelines for laboratory animal welfare and were approved by the Ethics Committee of Beijing Hospital of Traditional Chinese Medicine affiliated to Capital Medical University (Beijing, China) (Ethics No. BJTCM-M-2021-06-01).

Histopathological Analysis

The mouse skin tissue was fixed with 4% paraformaldehyde solution for at least 24 h. The fixed skin tissue was embedded in paraffin and cut into 5 μm thick sections for histological evaluation with hematoxylin-eosin (H&E) staining.

Table 1 Primer Sequences for HaCaT Keratinocyte Genes

Gene Name	Primer Sequence (5'–3' Direction)
IL-6	F: AGACAGCCACTCACCTCTTC
	R: ACCAGGCAAGTCTCCTCATT
IL-23A	F: AGTCAGTTCTGCTTGCAAAGG
	R: AGTAGGGAGGCATGAAGCTG
K17	F: TGAGGAGCTGCAGAACAAGA
	R: TCTGTAGCAGGATGTTGGCA
VEGF A	F: CTGTCTTGGGTGCATTGGAG
	R: ACCAGGGTCTCGATTGGATG
GAPDH	F: GTCGGAGTCAACGGATTTGG
	R: ATCTCGCTCCTGGAAGATGG

Table 2 Primer Sequences for Mice Genes

Gene Name	Primer Sequence (5'–3' Direction)
IL-17	F: CAGACTACCTCAACCGTTCCAC
	R: CAGCTTTCCCTCCGCATTGACA
IL-23	F: TAATGTGCCCCGTATCCAGTG
	R: GCTCCCCTTTGAAGATGTCAGA
K17	F: GGCCACCATGCAGAACCTCA
	R: CTTCACCTCCAGCTCAGTGTT
Actin	F: CTCCTGAGCGCAAGTACTCT
	R: TACTCCTGCTTGCTGATCCAC

The thickness of the skin was measured and calculated using Image Pro Plus 6.0 software. One representative site of each mouse and five regions of each representative site were randomly selected for histological analysis.

Statistical analysis

All experiments were repeated at least three times. GraphPad Prism 8 was used for data processing. Data are expressed as mean ± standard deviation (x ± s), and univariate analysis of variance (ANOVA) was used for the comparison of differences between groups. Differences with $P < 0.05$ were considered statistically significant.

Results and Discussion

Preparation and Characterization of GEN-Loaded Chitosan Nanoparticles

A schematic diagram of the synthesis of gentiopicroside-loaded chitosan nanoparticles (CHI-GEN) is shown in Figure 1. Hydroxyethylated chitosan nanoparticles were prepared, and then hydroxyethylated chitosan and GEN were self-assembled to form CHI-GEN.

Absorbance was measured using UV-vis spectrophotometer.

Figure 2 shows the UV absorption of GEN, CHI, and Chi-Gen. GEN showed absorption at 270 nm, while CHI had almost no absorption in the UV-visible region. CHI-GEN's absorption peak at 270 nm was significantly enhanced, indicating that GEN successfully loaded CHI.

Characterization Using Transmission Electron Microscopy

TEM was used to characterize the morphology and particle size of non-loaded CHI and CHI-GEN. As shown in Figure 3, both non-loaded CHI and CHI-GEN contained monodispersed and spherical particles, with an average particle size of approximately 30 nm for non-loaded CHI and 100 nm for CHI-GEN.

Particle Size and Zeta Potential Analysis

Hydration particle sizes of CHI and CHI-GEN were characterized using DLS (Figure 4). The hydration particle size distribution of non-loaded CHI was 40.6 ± 0.7nm and that of Chi-GEN was 117.6 ± 0.3nm. From empty CHI to CHI-GEN, the hydration particle size increased, indicating that CHI successfully loaded GEN to become CHI-GEN. The diameter obtained using DLS measurement was greater than that measured using TEM, which may be because DLS measured the hydration particle sizes of wet and extended nanoparticles, while TEM measured dry and contracted nanoparticles.

The zeta potential of GEN and CHI-GEN was detected using DLS (Figure 5). The zeta potential (surface charge) of GEN nanoparticles was −2.31 ± 0.41 mV. CHI had a small amount of amino on the outside; therefore, it had a positive charge. When CHI was coated with GEN, the potential was 2.69 ± 0.87 mV. CHI-GEN nanoparticles with positive charge can easily adhere to the negatively charged membrane due to electrostatic interaction force. The higher the zeta potential,
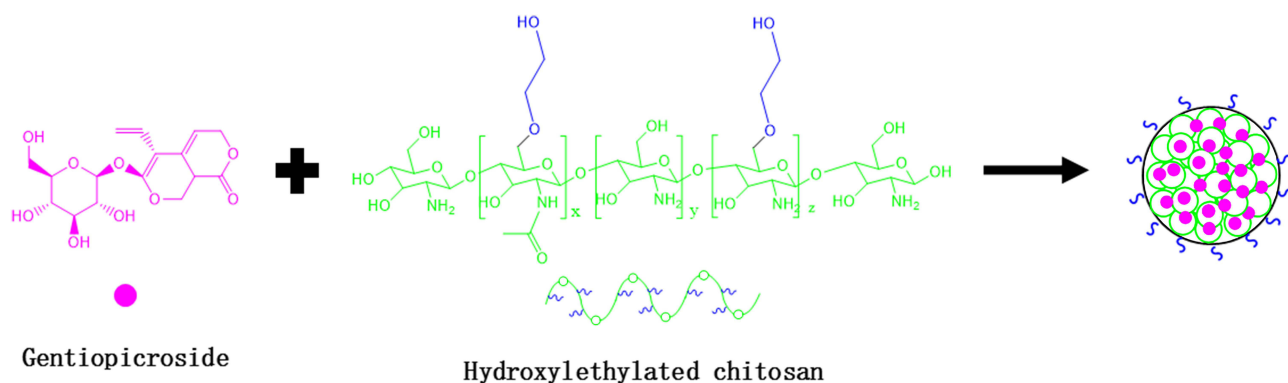

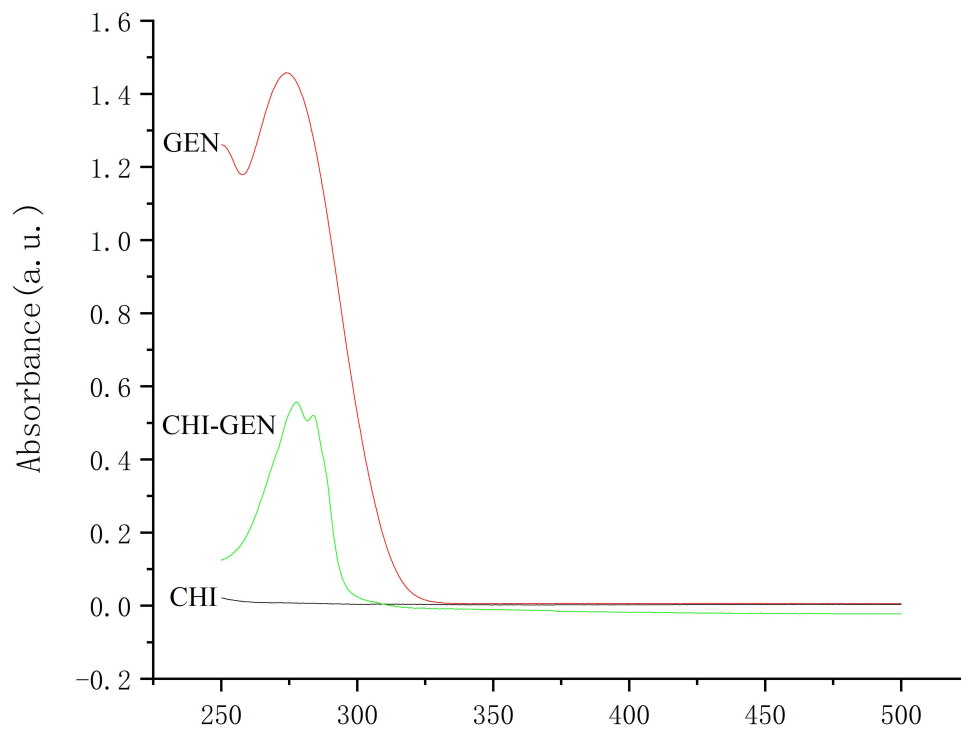**Figure 1** CHI-GEN synthesis diagram.

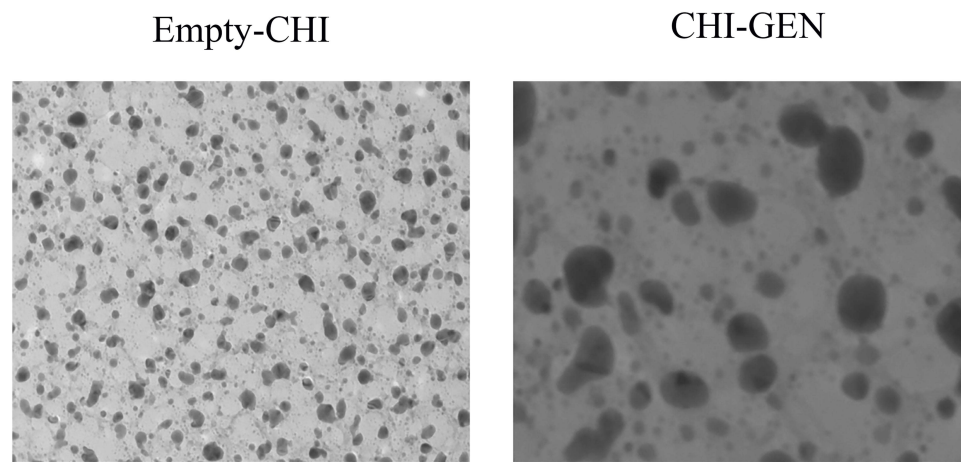**Figure 2** UV absorption of GEN, CHI, and CHI-GEN.

Figure 3 Micrographs of non-loaded CHI and CHI-GEN taken by TEM with scale bar = 100nm.

the greater the adhesion to the membrane. A positive charge is a sign of superior biological adhesion performance of nanomaterial systems, which is a prerequisite for topical drug delivery.

In vitro Drug Release Study

Release dynamics and behavior of GEN in CHI-GEN at room temperature in simulated human blood (pH 7.4) and simulated cellular lysosomes (pH 5.5) were evaluated. As shown in Figure 6, the release trend of GEN in both media was the same within 3 h, after which the release of GEN in the simulated cell lysosomes significantly increased. The 24 h cumulative release of GEN at pH 5.5 was 67.2%, which was much higher than at pH 7.4 (35%).

Whether nanoparticles can achieve controlled release of the encapsulated drugs is an important indicator of drug efficacy. In vitro drug release study showed that the 24 h release amount of GEN in CHI-GEN nanoparticles at pH7.4 was
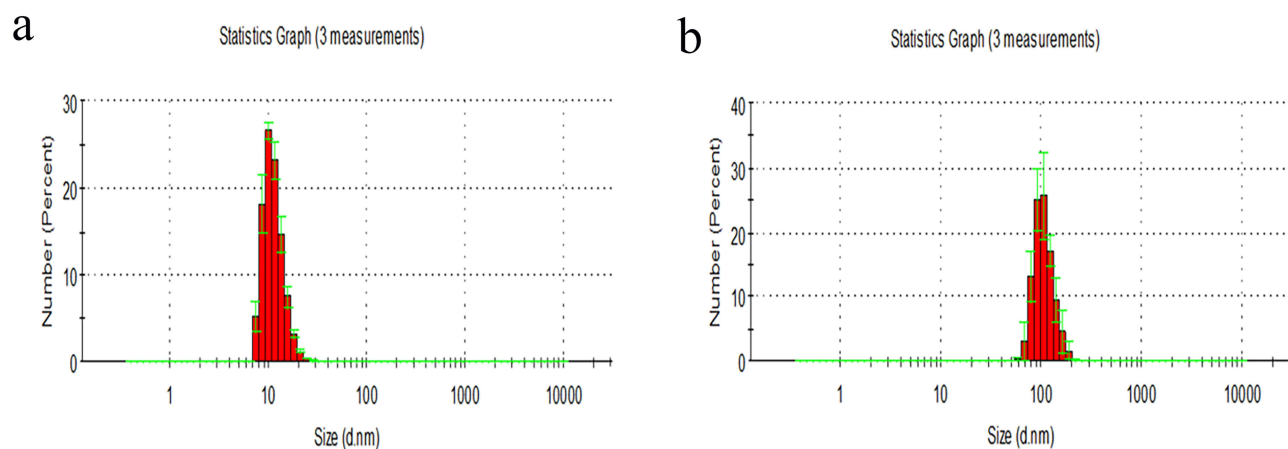
Figure 4 Hydration particle sizes of non-loaded CHI and CHI-GEN detected using DLS. (**a**) non-loaded CHI particle size and (**b**) CHI-GEN particle size.
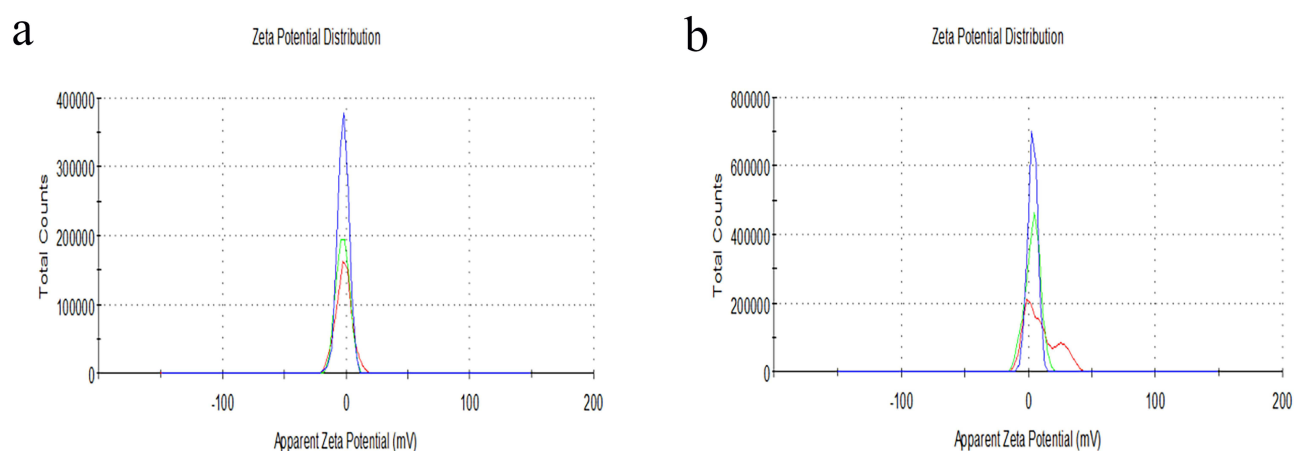

Figure 5 Zeta potential of GEN and CHI-GEN detected using DLS. (**a**) GEN Zeta potential (−2.31 ± 0.41 mV); (**b**) potential after CHI was coated with GEN (2.69 ± 0.87mV).

significantly lower than that at pH5.5, indicating that the drug release rate of CHI-GEN was significantly dependent on pH (increased with the decrease of pH). This may be because a decrease in pH increases the protonation of CHI, leading to dissociation of the electrostatic interaction between GEN and CHI, allowing more GEN to be released. This results in a reduction in the charge density of the crosslinker, causing the CHI to expand and release the trapped GEN. Studies on skin pH and psoriasis revealed that the pH of psoriasis patients (5.2 ± 0.5) is generally lower than that of healthy people (5.6 ± 0.5).[36] CHI can respond in slightly acidic conditions, and the topical application of CHI-loaded drugs in psoriasis is conducive to improving the utilization of drugs. CHI is an effective carrier for drug delivery in the biological environment and can be effectively used in the treatment of psoriasis.

Intracellular Uptake Study of CHI-GEN

Ingestion of nanocarriers by cells for successful uptake of loaded drugs is also another important indicator to test the performance of the nanocarriers. As shown in Figure 7, CHI can enter the cell at 3 h and is mainly located on the cell membrane. After incubation for 12 h, the green fluorescence signal of FITC-CHI inside the cells was enhanced indicating that the uptake of CHI by HaCaT cells was time-dependent. Next, we used lysosome specific fluorescent probe to examine the point of entry of CHI and observed the co-localization of FITC-CHI and lysosome with a confocal laser microscope. As shown in Figure 7, the co-localization of FITC-CHI and lysosome was very clear, indicating that FITC-CHI entered the lysosome. The pH of lysosome is approximately 5.0, which may lead to the release of CHI-GEN in the lysosome.
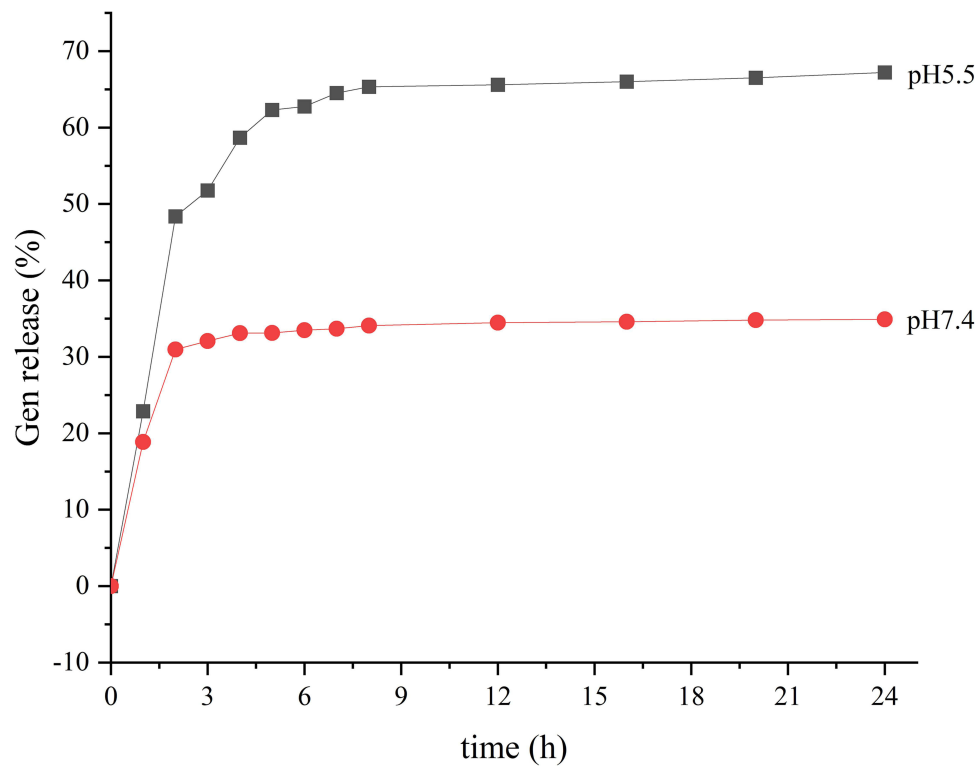
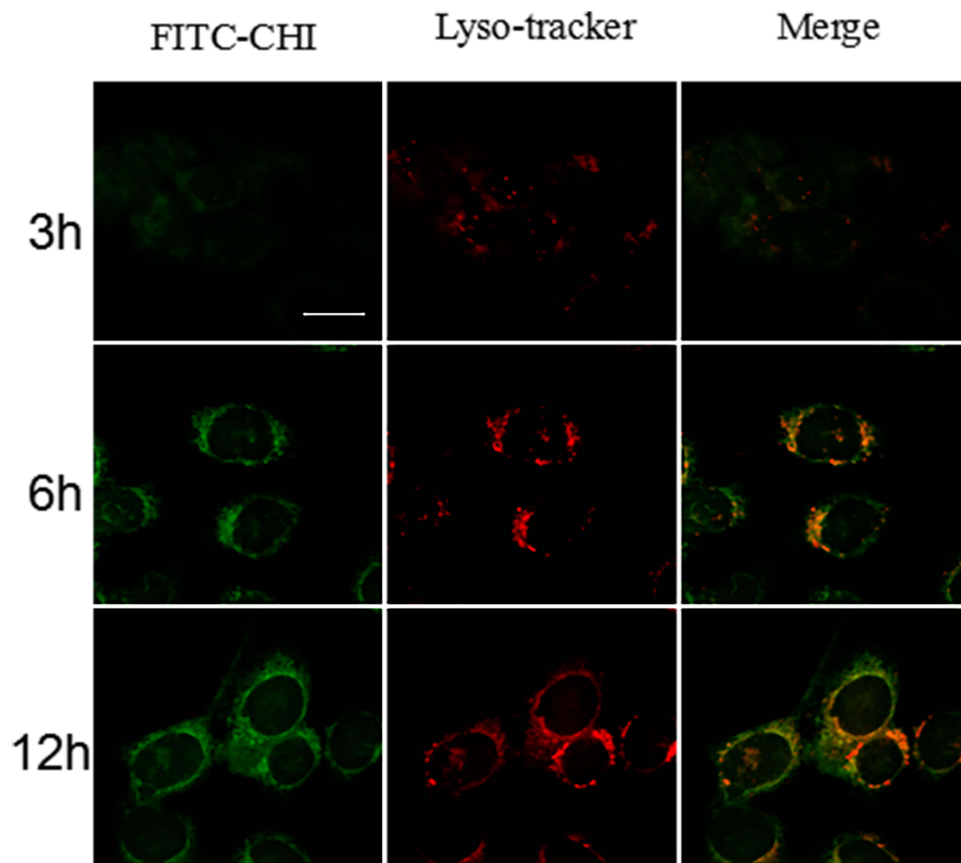**Figure 6** GEN release in vitro at different pH.

Figure 7 Co-localization of FITC-CHI particles and lysosomes Laser scanning confocal micrograph (100 ×) Scale bar =10 μM.

Combined with the results of in vitro drug release studies, we hypothesized that GEN in CHI-GEN nanoparticles was released slowly in the blood, and the nanoparticles would first enter the lysosome after entering the cell, and then were released into the cytoplasm or degraded in the lysosome, to achieve controlled release of GEN and improve the drug efficacy in local lesions.

These results indicate that CHI-GEN can be successfully ingested by cells. We further evaluated the mechanism of CHI-GEN entry into cells. Nanoparticles can enter mammalian cells in three ways: clathrin-mediated endocytosis, macropinocytosis, and petiolar protein-mediated endocytosis. As shown in Figure 8, after treatment of HaCaT cells with amiloride, a specific inhibitor of macropinocytosis, the intracellular fluorescence signal was reduced, indicating that CHI-GEN could not enter cells. Therefore, it can be concluded that CHI-GEN enters cells through macropinocytosis and rapidly releases GEN in the acidic environment of lysosomes to exert its anti-psoriasis effect.

In vitro Cytotoxicity Study

Drug carriers should be non-toxic to the target animal. HaCaT cells were treated with TNF-α at a concentration of 10 ng/mL to simulate the proliferation model of psoriasis, and the treated cells were exposed to CHI, GEN, and CHI-GEN NPs, and the cell viability was detected using MTT assay. As shown in Figure 9, CHI (6.25–800 ng/mL) did not affect the survival rate of HaCaT cells; therefore, CHI prepared by us was safe for HaCaT cells within a certain concentration. However, when the concentration of free GEN ≥50 ng/mL and CHI-GEN NPs ≥25 ng/mL, TNF-α-induced HaCaT cell viability was reduced and the inhibitory effect was enhanced with an increase in concentration ($p < 0.05$). The inhibitory effect of 50 ng/mL CHI-GEN NPs and 200 ng/mL GEN on the survival rate of HaCaT cells was comparable, and this concentration was selected for subsequent experiments ($p < 0.05$). Free GEN had low cytotoxicity due to its low bioavailability, while CHI-GEN NPs exhibit stronger cytotoxicity at lower doses due to better uptake by cells.
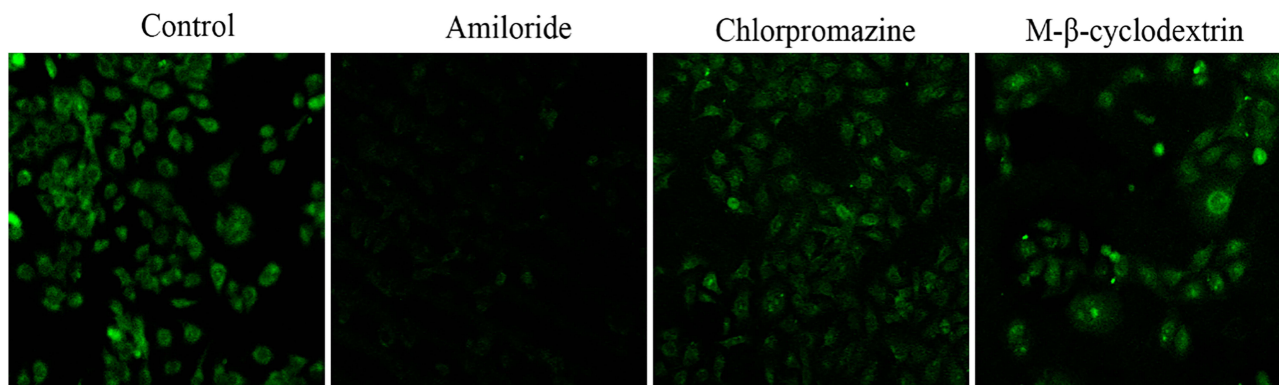

Figure 8 Uptake of CHI-GEN nanoparticles by HaCaT cells Laser scanning confocal microscope (10 ×) Scale bar = 50 μM.
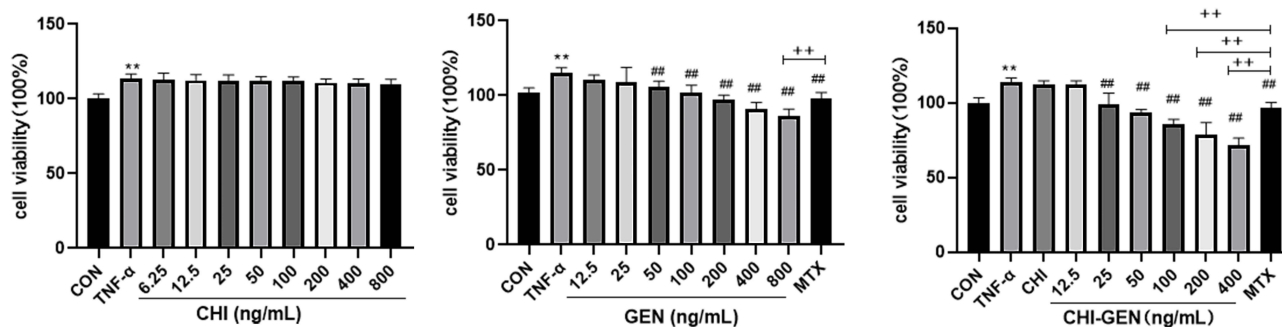

Figure 9 The effects of different drugs (CHI, GEN, CHI-GEN) on TNF-α -induced HaCaT cell viability expressed as mean ± SD, n = 6, and the differences were evaluated using ANOVA. Compared with control group,**$p < 0.01$; Compared with TNF-α treated model group, ##$p < 0.01$; Compared with MTX treated control group,++$p < 0.01$.

Table 3 Effect of CHI-GEN on Apoptosis of HaCaT Cells Induced by TNF-α

Group	Apoptosis Rate (100%)
Control	9.86 ± 1.15
Model	5.08 ± 0.75
MTX	10.53 ± 1.28
CHI	6.70 ± 0.52
GEN	7.0 ± 1.61
CHI-GEN	12.61 ± 2.58

CHI-GEN Reduced the Effect of TNF-α-Induced HaCaT Keratinocyte Hyperproliferation and Inflammatory Cytokine Expression

The balance between keratinocyte proliferation and apoptosis is critical for maintaining skin homeostasis. This balance is disrupted in psoriatic lesions.[37] Monolayer keratinocyte culture is widely used in biological and pharmacological studies and screening of anti-psoriasis drugs. In this study, we used TNF-α to induce HaCaT cells to establish the psoriasis proliferation model. To determine whether CHI-GEN could inhibit proliferation and promote apoptosis, HaCaT cells were seeded in 96-well plates and differently treated.

The apoptosis of HaCaT cells was significantly inhibited in the model group compared with the blank control group. CHI-GEN group and MTX group showed increased apoptosis compared with model group ($p < 0.05$), and CHI-GEN and MTX promoted apoptosis equally ($p > 0.05$) (Table 3, Figures 10 and 11). These results suggest that CHI-GEN can improve the psoriasis-like excessive proliferation of HaCaT cells induced by TNF-α and promote their apoptosis. However, the relationship between CHI-GEN regulation of keratin 17 and other differentiation markers remains to be further studied.

Keratin 17 is overexpressed in the epidermis of psoriasis.[38] Changes in keratinocyte differentiation in psoriasis are characterized by upregulation of the early differentiation marker keratin 17.[39] K17 has pro-proliferation and pro-inflammatory effects on keratinocytes,[40] thus participating in the pathogenesis of psoriasis.
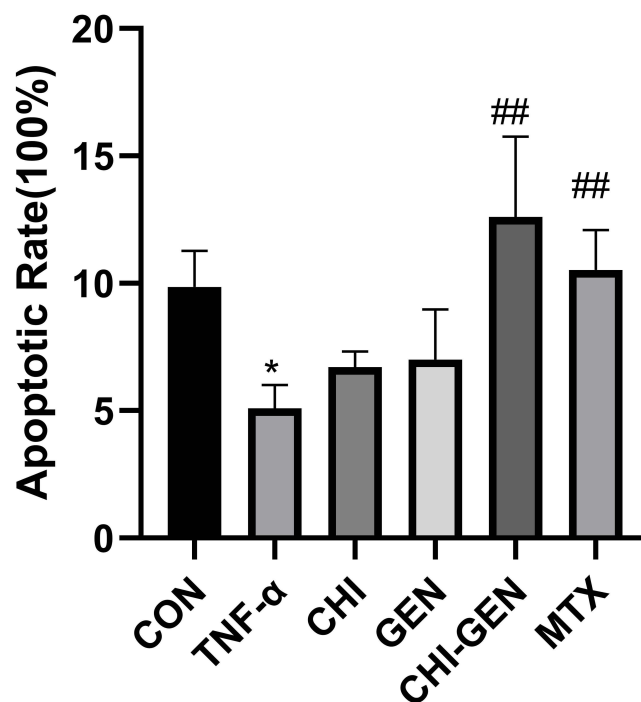

Figure 10 Effects of GEN and CHI-GEN on TNF-α-induced apoptosis of HaCaT cells. Data are expressed as mean ± SD, n = 3, and the differences were evaluated using ANOVA. Compared with control group, *p<0.05; compared with TNF-α treated model group, ##p<0.01; compared with MTX treated control group.
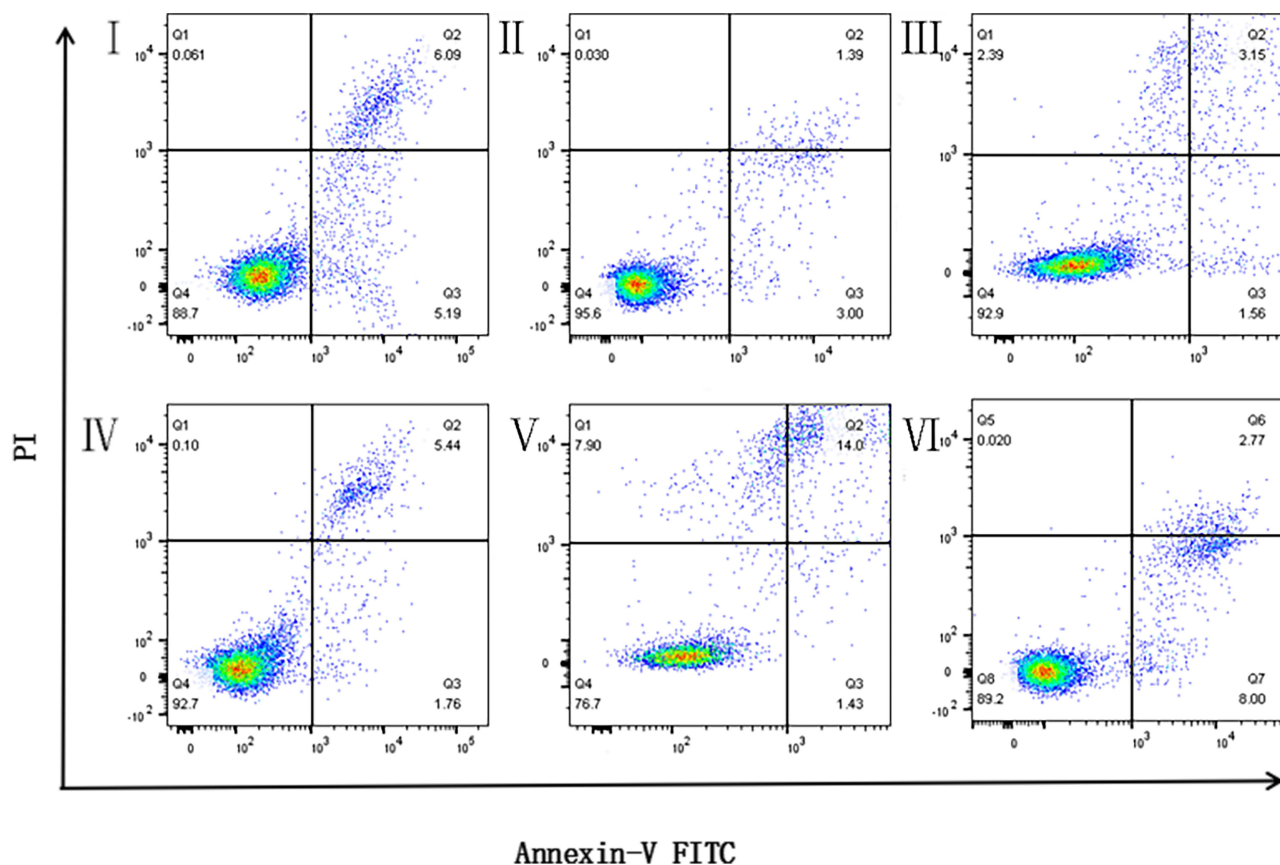
Figure 11 Effect of CHI-GEN on TNF-α -induced apoptosis of HaCaT cells was detected using flow cytometry. I: Control Group; II: Model Group TNF- α (10 ng/mL); III: TNF- α (10 ng/mL) + GEN (200 ng/mL); IV: TNF- α (10 ng/mL) + CHI (50 ng/mL); V: TNF- α (10 ng/mL) + CHI-GEN (50 ng/mL); VI: TNF- α (10 ng/mL) + MTX (5 mg/L).

Keratinocytes are both participants and victims in the pathogenesis of psoriasis.[41–43] Studies have shown that activated keratinocytes secrete abundant cytokines, including IL-6, IL-17, and IL-23.[9] Il-23 and IL-17 can induce related inflammatory pathways and enhance tissue inflammation.[44,45] As a downstream mediator of IL-17A, IL-6 cooperates with IL-17A to promote the production of proinflammatory cytokines by keratinocytes.[46]

As shown in Table 4 and Figure 12, the mRNA expression levels of inflammatory cytokines (IL-6 and IL-23A) and vascular growth factor (VEGF) in HaCaT cells treated with CHI-GEN, GEN, and MTX were significantly reduced compared with the

Table 4 The Levels of Target mRNA Detected Using PCR After Drug Intervention

Group	IL-6	IL-23A	K17
Model	2.69 ± 0.96	2.56 ± 0.53	2.73 ± 0.62
CHI	2.90 ± 0.58	1.98 ± 0.17	3.40 ± 0.40
GEN	0.96 ± 0.22	1.30 ± 0.18	1.82 ± 0.26
CHI-GEN	0.60 ±0.05	0.75 ± 0.06	1.58 ± 0.24
MTX	1.03 ± 0.11	0.70 ± 0.15	1.19 ± 0.09

Abbreviations: GEN, Gentiopicrin; CHI, Chitosan; CHI-GEN, Gentiopicroside-loaded chitosan nanoparticles; FITC-CHI, FITC-loaded chitosan nanoparticles; HaCaT, human-immortalized keratinocytes; TNF-α, tumor necrosis factor-α; MTT, 3-(4,5-Dimethylthiazol-2-yl)-2,5-diphenyltetrazolium bromide;K17, keratin 17; VEGF, vascular endothelial growth factor; Interleukin 6, IL-6; Interleukin 23A, IL-23A; Interleukin 17A, IL-17A; qRT-PCR, quantitative Real-time Polymerase Chain Reaction; IMQ, Imiquimod; PASI, psoriasis area severity index; H&E, hematoxylin-eosin; MEM, Minimum essential medium; FBS, fetal bovine serum; TRY, trypsin-EDTA solution; MTX, methotrexate; TAC, Tacrolimus; PBS, Phosphate-buffered saline; DMSO, Dimethyl sulfoxide; PVDF, Polyvinyl difluoride; GAPDH, Glyceraldehyde-3-phosphate dehydrogenase; TEM, transmission electron microscopy; DLS, dynamic light scattering.
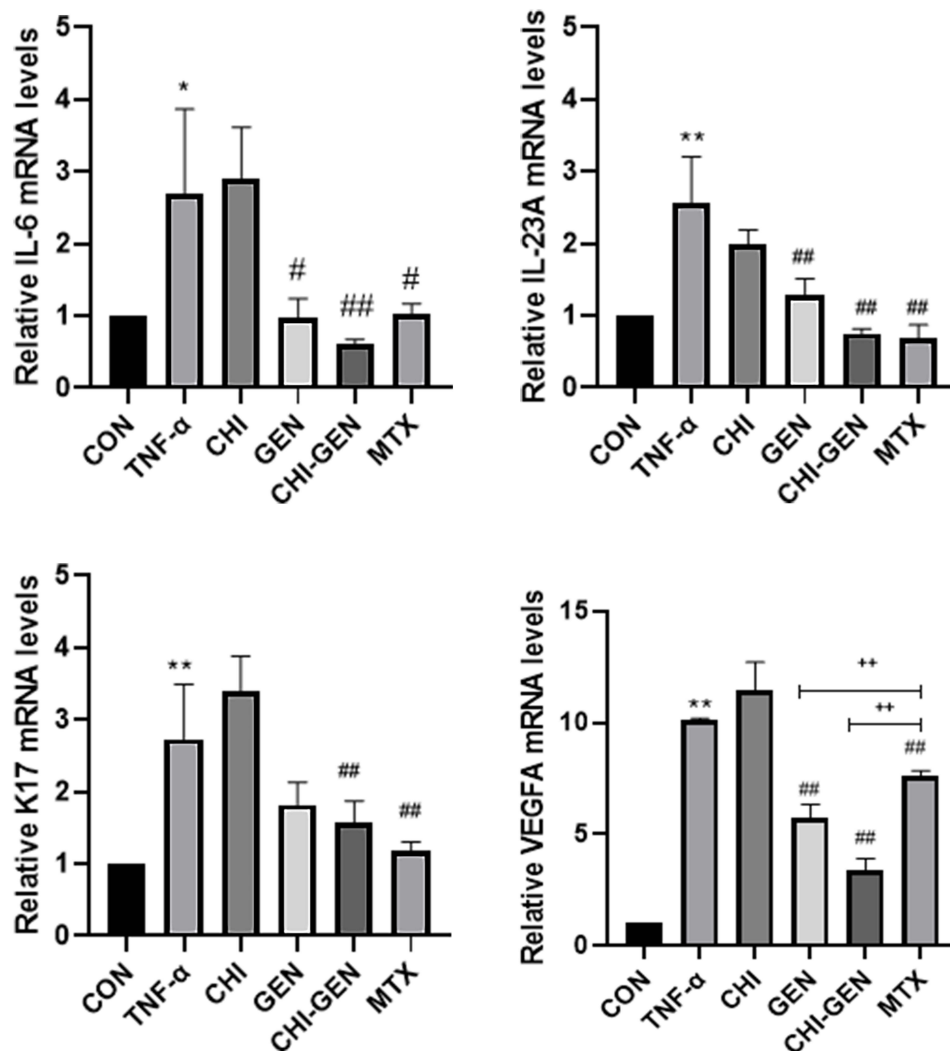
Figure 12 Effect of different drugs on relative mRNA expression level of HaCaT cells. Data are expressed as mean ± SD, n = 3, and the differences were evaluated using ANOVA. Compared with control group, *$p < 0.05$, **$p < 0.01$; compared with TNF-α treated model group, #$p < 0.05$, ##$p < 0.01$; compared with MTX treated control group, ++$p < 0.01$.

TNF-α treated model group, and the mRNA levels of IL-6 and VEGF in the CHI-GEN group were lower than those in the MTX group. Additionally, the level of K17 mRNA was also partially decreased after treatment with CHI-GEN and MTX.

qRT-PCR analysis showed that TNF-α activated keratinocyte proliferation, induced inflammatory response, and increased the expression of IL-6, IL-17, IL-23 and other genes actively involved in the inflammatory cascade. CHI-GEN attenuates the upregulation of inflammatory cytokines including IL-6, IL-23, and IL-17 in TNF-α-induced HaCaT cells. These results suggest that CHI-GEN can ameliorate the inflammatory state of TNF-α-induced psoriatic HaCaT cells.

Angiogenesis induced by vascular endothelial growth factor is one of the characteristics of psoriasis, and the severity of psoriasis is related to the level of serum vascular endothelial growth factor.[47,48] Overexpression of VEGF in skin biopsied from patients with psoriasis suggests a link between epidermal VEGF levels and keratinocyte proliferation. Therefore, we investigated the effect of GEN and CHI-GEN on the expression of vascular growth factor VEGF in keratinocytes. The results showed that CHI-GEN treatment may improve psoriasis-like angiogenesis.

CHI-GEN Cream Improves Psoriatic Dermatitis Induced by IMQ in Mice

To further confirm the anti-psoriasis effect of CHI-GEN, we prepared CHI-GEN cream and established the animal model of psoriasis by topical application of imiquimod cream[35,49] and corresponding creams of each experimental group on
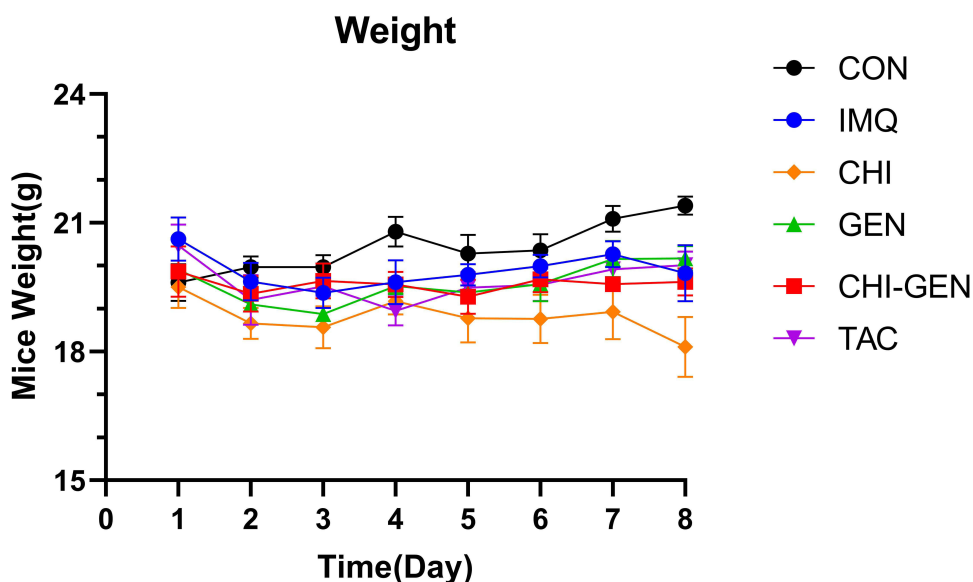
Weight

Figure 13 Body weight of mice in each group was continuously monitored from day 1 to 8.

BALB/c mice for 7 consecutive days. We preliminarily assessed the safety of this ointment (6% concentration) (Figure 13). Compared with the control group, the mice in the CHI-GEN and GEN groups did not show any significant decrease in weight, and could drink, eat and move normally, which indicated that the cream had no obvious toxicity. The severity of psoriasis-like inflammation in mice is shown in Figures 14 and 15. Scales and erythema on the back of mice in the model group gradually worsened on the third day of the experiment. The skin lesions were particularly severe on the seventh day showing large areas of erythema and scales. Compared with the model group, psoriasis-like symptoms such as erythema and scales were significantly reduced in the GEN group and the CHI-GEN group, showing the same reduction trend as the TAC group, while the skin of the blank group remained unchanged (Figure 14).

From day 3, PASI score (Figure 15) showed that except for the blank group, the scores of other groups increased to varying degrees as the experiment progressed. However, the scores of the treatment group were lower than those of the model group, indicating that the psoriasis mice model was successfully established. From day 5, the total scores of erythema, scale, induration and PASI in CHI-GEN group, GEN group and TAC group were lower than those in model group. On day 8, the scores of CHI-GEN group and TAC group were lower than those of model group, and scores in the CHI-GEN group were lower than those in the GEN group. The total and erythema scores in the CHI-GEN group were lower than those in the GEN group.

This indicates that GEN, CHI-GEN, and TAC cream could inhibit the psoriatic symptoms in this model, and CHI-GEN had better effect anti-psoriatic effect than GEN.

CHI-GEN Cream Can Alleviate Histopathological Changes of Psoriasis-Like Lesions in Mice Induced by Imiquimod

HE staining showed (Figure 16) that the skin tissue status of the CON, IMQ, GEN, CHI-GEN and TAC groups were significantly different. Compared with the control group, the epidermis of the skin on back of mice in the model group was thickened ($p < 0.01$), and there were incomplete keratinized keratinocytes in the cuticle, accompanied by micro-abscesses, indicating that the model was successfully established.

Compared with model group, the parakeratosis and microabscess were alleviated to some extent in CHI, GEN, CHI-GEN, and TAC groups. Meanwhile, CHI-GEN and TAC groups showed a reduction in skin thickness ($p < 0.05$), while the other groups had no statistical difference in skin thickness ($p > 0.05$) (Figure 17). These results suggest that CHI-GEN cream could effectively delay the occurrence of psoriasis-like skin inflammation in mice and improve the progression of IMQ-induced psoriasis.
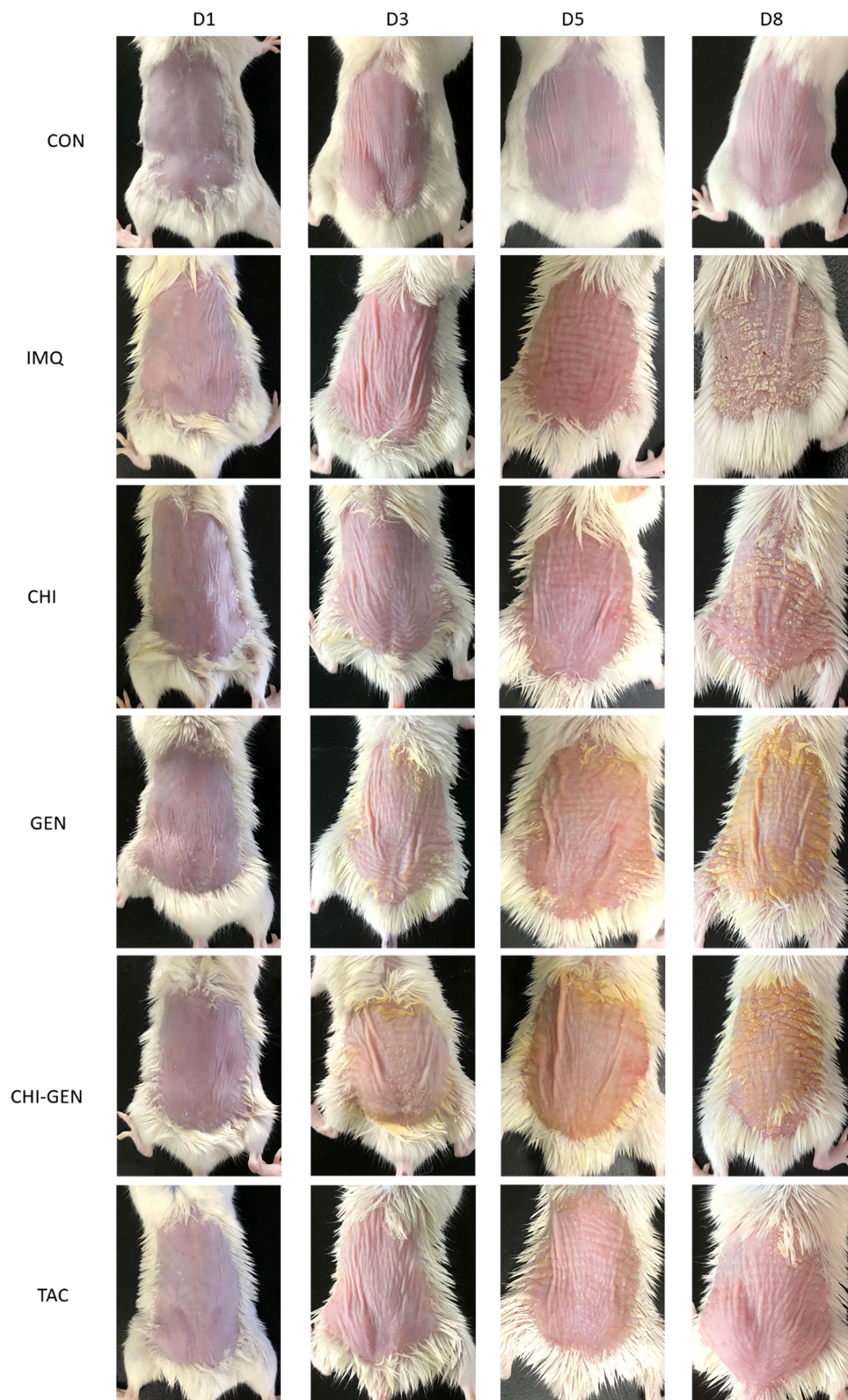
Figure 14 Effect of CHI-GEN on imQ-induced psoriasis-like lesions in mice. The macroscopic appearance of mouse back skin on days 1, 3, 5 and 8.
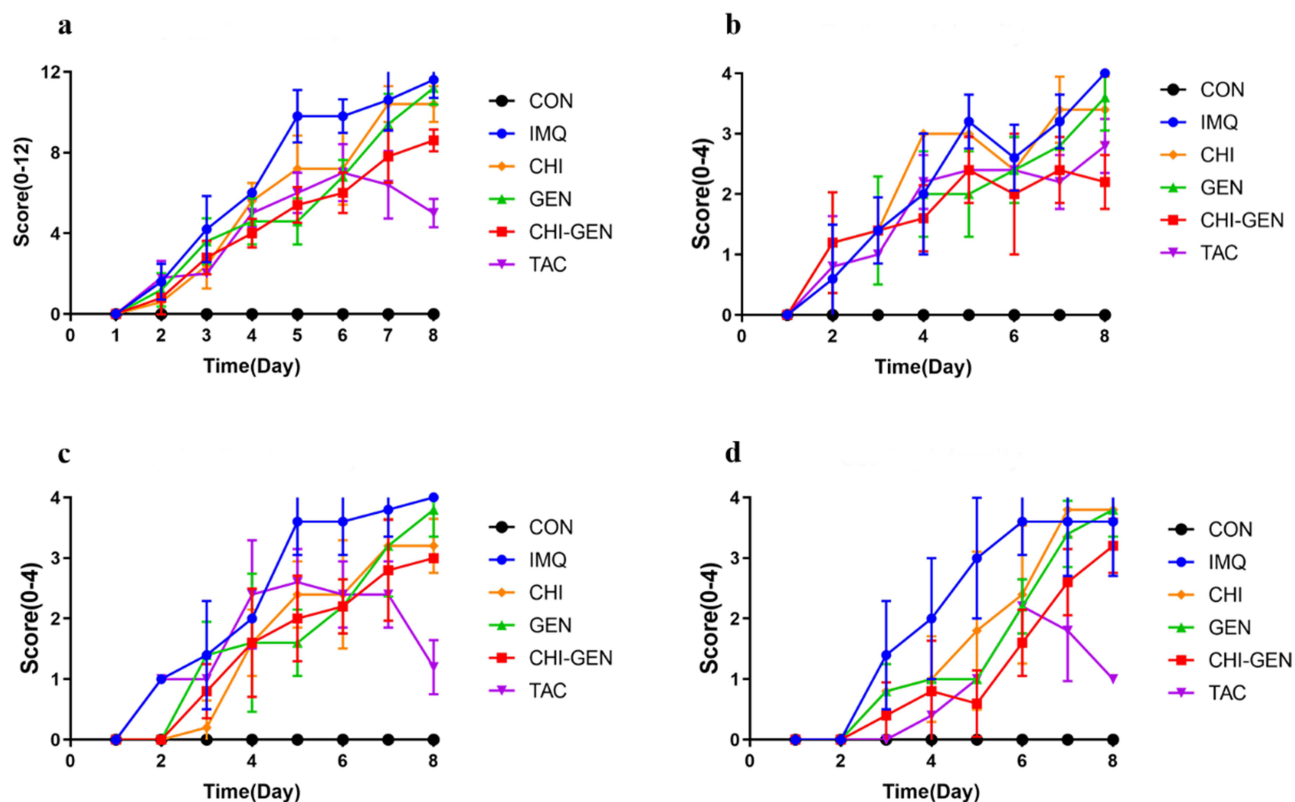
Figure 15 Skin changes on the back of mice were scored according to PASI at days 1–8, including (**a**) total PASI score, (**b**) erythema, (**c**) induration, and (**d**) scaling.

CHI-GEN Cream Can Reduce the mRNA Expression of Cytokines K17, IL-17A and IL-23 in IMQ-Induced Psoriatic Lesions in Mice

On day 8, qRT-PCR was performed using RNA isolated from the back skin of mice. As shown in Figure 18, compared with the control group, the mRNA expression levels of IL-17A, IL-23, and K17 in the skin of model group (IMQ) were significantly increased, indicating that psoriatic lesions of mice can secrete cytokines with application of IMQ. Compared with model (IMQ) group, the mRNA levels of IL-17A and IL-23 were decreased in GEN group, CHI-GEN group, and TAC group ($p < 0.05$). These results suggest that GEN and CHI-GEN can inhibit the expression of inflammatory factors in mice psoriasis lesions. The expression of K17 mRNA in skin of GEN group and CHI-GEN group decreased, indicating that GEN and CHI-GEN could inhibit keratinocyte proliferation and differentiation. However, the mRNA expression of IL-17A, IL-23 and K17 in the matrix group were not significantly different, indicating that the matrix group had no significant anti-inflammatory and inhibitory effects on differentiation. However, there was no statistical difference in the mRNA expression of these cytokines in the CHI group. We believe that the anti-inflammatory and anti-differentiation effects of CHI were not obvious. Combined with the above discussion in 2.5, IL-17A and IL-23 are proinflammatory cytokines produced by keratinocytes, which can induce related inflammatory pathways and enhance tissue inflammation [48, 50–52]. K17 is characteristic of altered differentiation of psoriatic keratinocytes and is an early differentiation marker [43]. These results suggest that CHI-GEN can ameliorate psoriasis-like skin lesions and inflammatory state induced by IMQ in mice. We think this might be related to the inhibition of keratinocyte inflammatory cytokines IL-17, IL-23 and keratinocyte proliferation protein K17.
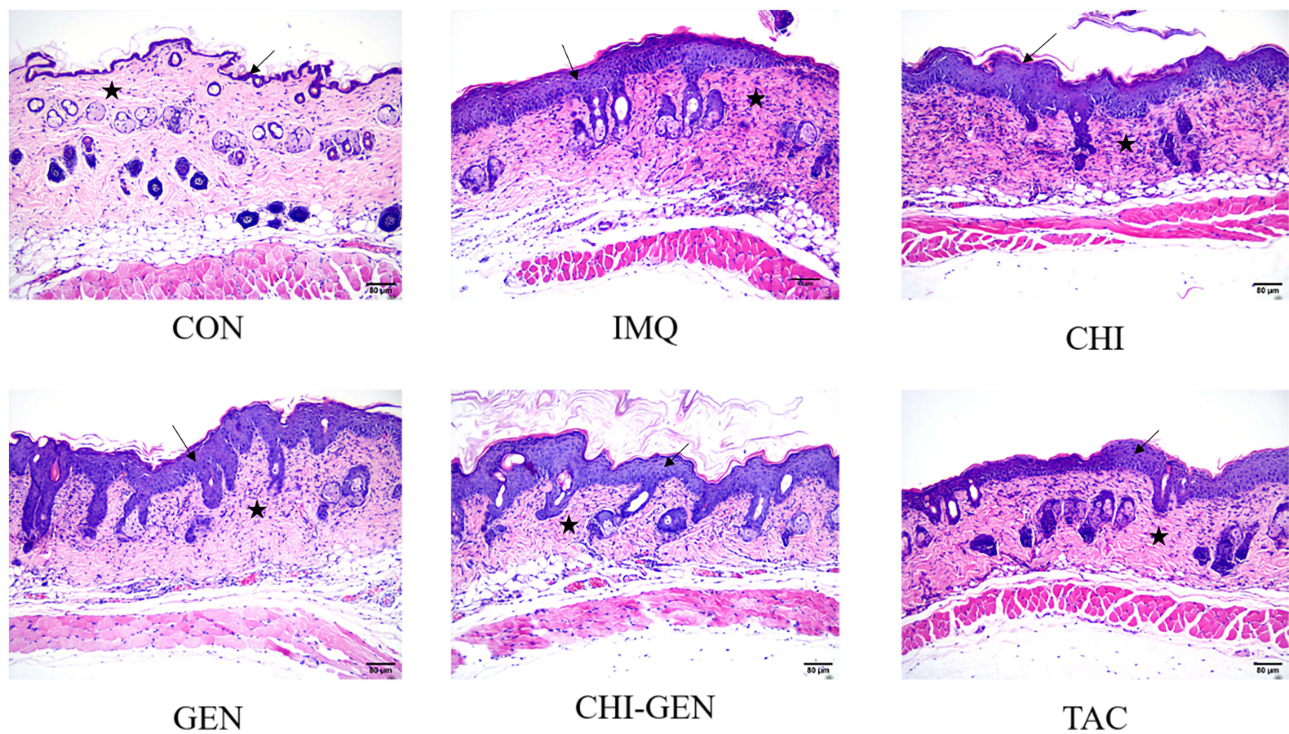
Figure 16 Histopathological observation of H&E staining of mice dorsal skin showing changes in epidermal thickness and morphology. Black arrows: epidermal layer, stars: dermal layer (× 400).
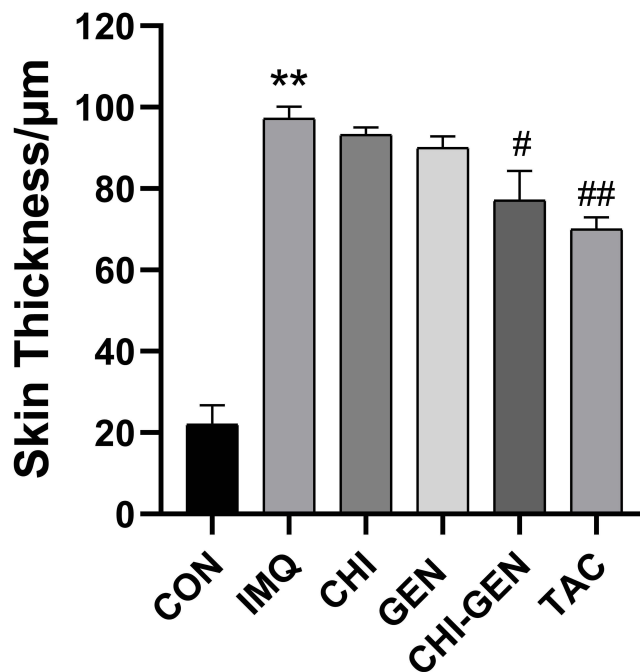

Figure 17 Back skin thickness of mice. The skin thickness was calculated using Image-Pro Plus 6.0, data are presented as mean ± SD (n = 3), and the differences were evaluated using ANOVA. Compared with CON group, **$p < 0.01$; Compared with IMQ group, #$p < 0.05$, ##$p < 0.01$.
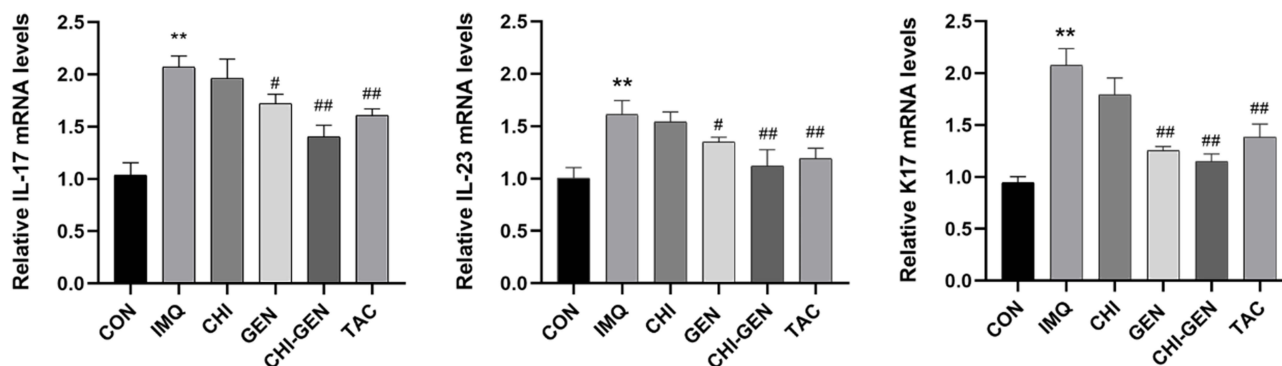
Figure 18 The relative mRNA expression of related cytokines (IL-17A, IL-22, and IL-23) in IMQ-induced psoriatic skin of mice. Data are presented as mean ± SD, n = 3, and differences were assessed using ANOVA. Compared with CON group, ** $p<0.01$; Compared with IMQ group, # $p<0.05$, ## $p<0.01$.

Conclusion

Psoriasis is a chronic recurrent disease that seriously affects the quality of life of patients.[50] Its pathogenesis has not been fully elucidated and the existing treatment methods have limitations and side effects. Therefore, it is very important to find new therapeutic drugs.[51,52] In this study, the properties of gentiopicrin-loaded chitosan nanoparticles were examined and biological evaluation was carried out.

The results showed that gentiopicroside has anti-proliferation, apoptosis-promoting, anti-inflammatory, and anti-angiogenic effects in in vitro and in vivo psoriasis models. The acid sensitivity and targeting ability of chitosan drug delivery system limits the concentration of drugs entering systemic circulation and maximizes the drug concentration in skin lesion cells. Therefore, chitosan can improve the utilization of gentiopicrin while retaining the activity of free gentiopicrin. In conclusion, gentiopicrin-loaded chitosan nanoparticles are new and potentially effective drug delivery method with anti-psoriatic activity in IMQ-induced psoriatic skin inflammation model in Balb/c mice and in vitro cell culture.

Further studies on the anti-psoriasis activity of gentiopicroside-loaded chitosan particles in other cell and animal models, as well as the transdermal absorption rate and anti-psoriasis mechanism of gentiopicroside-loaded chitosan particles will be conducted.

Acknowledgments

Disclosure

The authors report no conflicts of interest in this work.

References

1. Griffiths CE, Armstrong AW, Gudjonsson JE, Barker JN. Psoriasis. *Lancet*. 2021;397(10281):1301–1315. doi:10.1016/S0140-6736(20)32549-6
2. Armstrong AW, Read C. Pathophysiology, Clinical presentation, and treatment of psoriasis: a review. *JAMA*. 2020;323(19):1945–1960. doi:10.1001/jama.2020.4006
3. Takeshita J, Grewal S, Langan SM, et al. Psoriasis and comorbid diseases: epidemiology. *J Am Acad Dermatol*. 2017;76(3):377–390. doi:10.1016/j.jaad.2016.07.064
4. Alqassimi S, Albrashdi S, Galadari H, Hashim MJ. Global burden of psoriasis – comparison of regional and global epidemiology, 1990 to 2017. *Int J Dermatol*. 2020;59(5):566–571. doi:10.1111/ijd.14864
5. Garzorz-Stark N, Eyerich K. Psoriasis Pathogenesis: keratinocytes Are Back intheSpotlight. *J Invest Dermatol*. 2019;139(5):995–996. doi:10.1016/j.jid.2019.01.026
6. Rendon A, Schäkel K. Psoriasis Pathogenesis and Treatment. *Int J Mol Sci*. 2019;20(6):1475. doi:10.3390/ijms20061475
7. Armstrong AW, Read C. Pathophysiology, Clinical presentation, and treatment of psoriasis. a review. *JAMA J Am Med Assoc*. 2020;323(19):1945–1960.
8. Alcantara C, Reiche E, Simo A. Cytokines in psoriasis. *Adv Clin Chem*. 2020;100:171–204.
9. G K, B A, E C, S R. Therapeutics targeting the IL-23 and IL-17 pathway in psoriasis. *Lancet*. 2021;397(10275):754–766. doi:10.1016/S0140-6736(21)00184-7

10. Reich K, Gooderham M, Thaçi D, Crowley JJ, Paul C. Risankizumab compared with Adalimumab in patients with moderate-to-severe plaque psoriasis (IMMvent): a randomised, double-blind, active-comparator-controlled Phase 3 trial. *Lancet*. 2019;394(10198):576–586. doi:10.1016/S0140-6736(19)30952-3

11. Warren RB, Blauvelt A, Bagel J, et al. Bimekizumab versus adalimumab in plaque psoriasis. *New Engl J Med*. 2021;385(2):130–141. doi:10.1056/NEJMoa2102388

12. Ópez NG, Arnal CL, Perez JJ, Wagner EF. Topical application of an amygdalin analogue reduces inflammation and keratinocyte proliferation in a psoriasis mouse model. *Exp Dermatol*. 2021;30(11):1662–1674. doi:10.1111/exd.14390

13. Zhang M, Li N, Cai R, et al. Rosmarinic acid protects mice from imiquimod induced psoriasis-like skin lesions by inhibiting the IL-23/Th17 axis via regulating Jak2/Stat3 signaling pathway. *Phytother Res*. 2021;35(8):4526–4537. doi:10.1002/ptr.7155

14. Elgewelly MA, Elmasry SM, Sayed N, Abbas H. Resveratrol-loaded vesicular elastic nanocarriers gel in imiquimod-induced psoriasis treatment: in vitro and in vivo evaluation. *J Pharm Sci-Us*. 2021;111(2):417–431.

15. Huang TH, Lin CF, Alalaiwe A, Yang SC, Fang JY. Apoptotic or antiproliferative activity of natural products against keratinocytes for the treatment of psoriasis. *Int J Mol Sci*. 2019;20(10):2558. doi:10.3390/ijms20102558

16. Zhang X, Zhan G, Jin M. Botany, traditional use, phytochemistry, pharmacology, quality control, and authentication of Radix Gentianae Macrophyllae-A traditional medicine: a review. *Phytomedicine*. 2018;46:142–163. doi:10.1016/j.phymed.2018.04.020

17. Zhou D, Lv D, Zhang H. Quantitative analysis of the profiles of twelve major compounds in Gentiana straminea Maxim. Roots by LC-MS/MS in an extensive germplasm survey in the Qinghai-Tibetan plateau. *J Ethnopharmacol*. 2021;280:114068. doi:10.1016/j.jep.2021.114068

18. Wu S. Research Progress of Natural Product Gentiopicroside - a Secoiridoid Compound. Mini reviews in medicinal chemistry. *J Int Med*. 2017;17(1):62–77.

19. L Q, C L, M A, X L, Q J. Gentiana rigescensGentiopicroside, a Secoiridoid Glycoside from Franch, Extends the Lifespan of Yeast via Inducing Mitophagy and Antioxidative Stress. *Oxid Med Cell Longev*. 2020;2020:9125752. doi:10.1155/2020/9125752

20. J N, M H, Z T, et al. Gentiopicroside attenuates collagen-induced arthritis in mice via modulating the CD147/p38/NF-κB pathway. *Int Immunopharmacol*. 2022;108:108854. doi:10.1016/j.intimp.2022.108854

21. Almukainzi MA, El-Masry TA, Negm W, et al. Gentiopicroside PLGA Nanospheres: fabrication, in vitro Characterization, Antimicrobial Action, and in vivo Effect for Enhancing Wound Healing in Diabetic Rats. *Int J Nanomed*. 2022;17:1203–1225.

22. Zhang QL, Peng-Fei XI, Xue-Jing PE, et al. Synthesis, and anti-inflammatory activities of gentiopicroside derivatives. *Chin J Nat Medicines*. 2022;20(4):309–320. doi:10.1016/S1875-5364(22)60187-0

23. J M, F H, W Y, et al. Gentiopicroside Ameliorates Oxidative Stress and Lipid Accumulation through Nuclear Factor Erythroid 2-Related Factor 2 Activation. *Oxid Med Cell Longev*. 2020;2020:2940746. doi:10.1155/2020/2940746

24. Gao Y, Zhang X, Jin X. Preparation and Properties of Minocycline-Loaded Carboxymethyl Chitosan Gel/Alginate Nonwovens Composite Wound Dressings. *Mar Drugs*. 2019;17(10):575. doi:10.3390/md17100575

25. Kou SG, Peters L, Mucalo M. Chitosan: a review of molecular structure, bioactivities and interactions with the human body and micro-organisms. *Carbohydrate Polymers*. 2022;282:119132. doi:10.1016/j.carbpol.2022.119132

26. Zhang Z, Tsai PC, Ramezanli T, Michniak-Kohn BB. Polymeric nanoparticles-based topical delivery systems for the treatment of dermatological diseases. *Wiley Interdiscip Rev Nanomed Nanobiotechnol*. 2013;5(3):205–218. doi:10.1002/wnan.1211

27. Ta Q, Ting J, Harwood S, Browning N, Al-Kassas R. Chitosan nanoparticles for enhancing drugs and cosmetic components penetration through the skin. *Eur J Pharm Sci*. 2021;8:105765. doi:10.1016/j.ejps.2021.105765

28. Fereig SA, El-Zaafarany GM, Arafa MG, Abdel-Mottaleb M. Tacrolimus-loaded chitosan nanoparticles for enhanced skin deposition and management of plaque psoriasis. *Carbohyd Polym*. 2021;268(5):118238. doi:10.1016/j.carbpol.2021.118238

29. Ahmed N, Khan D, Rehman AU, Elaissari A, Ahmed N. Development and in vitro/in vivo Evaluation of pH-Sensitive Polymeric Nanoparticles Loaded Hydrogel for the Management of Psoriasis. *Nanomaterials-Basel*. 2021;11(12):3433. doi:10.3390/nano11123433

30. Cordenonsi LM, Faccendini A, Catanzaro M, Bonferoni MC, Ferrari F. The role of chitosan as coating for Nanostructured Lipid Carrier for skin delivery of fucoxanthin. *Int J Pharmaceut*. 2019;567:118487. doi:10.1016/j.ijpharm.2019.118487

31. Soares R, Campos M, Ribeiro G, et al. Development of a chitosan hydrogel containing flavonoids extracted from Passiflora edulis leaves and the evaluation of its antioxidant and wound healing properties for the treatment of skin lesions in diabetic mice. *J Biomed Mater Res A*. 2020;108(3):654–662. doi:10.1002/jbm.a.36845

32. Hatem S, Elkheshen SA, Kamel AO, et al. Functionalized chitosan nanoparticles for cutaneous delivery of a skin whitening agent: an approach to clinically augment the therapeutic efficacy for melasma treatment. *Drug Deliv*. 2022;29(1):1212–1231. doi:10.1080/10717544.2022.2058652

33. Ae A, Rrib C. Span 80/TPGS modified lipid-coated chitosan nanocomplexes of Acyclovir as a topical delivery system for viral skin infections. *Int J Pharmaceut*. 2021;609:121214.

34. Han L, Du LB, Kumar A, et al. Inhibitory effects of trolox-encapsulated chitosan nanoparticles on tert-butylhydroperoxide induced RAW264.7 apoptosis. *Biomaterials*. 2012;33(33):8517–8528. doi:10.1016/j.biomaterials.2012.07.034

35. Van D, Mourits S, Voerman J, et al. Imiquimod-Induced Psoriasis-Like Skin Inflammation in Mice Is Mediated via the IL-23/IL-17 Axis. *J Immunol*. 2009;182(9):5836. doi:10.4049/jimmunol.0802999

36. Cannavo S, Guarneri F, Giuffrida R, Aragona E, Guarneri C. Evaluation of cutaneous surface parameters in psoriatic patients. *Skin Res Technol*. 2017;23(1):41–47. doi:10.1111/srt.12299

37. B M, L AT. Keratinocyte-Polyamines and Dendritic Cells: a Bad Duet for Psoriasis. *Immunity*. 2020;53(1):16–18. doi:10.1016/j.immuni.2020.06.015

38. Zhang X, Yin M, Zhang LJ. Keratin 6, 16 and 17—Critical Barrier Alarmin Molecules in Skin Wounds and Psoriasis. *Cells-Basel*. 2019;8(8):807.

39. Florian E, Heinz F, Lutz L, et al. Differential Evolution of the Epidermal Keratin Cytoskeleton in Terrestrial and Aquatic Mammals. *Mol Biol Evol*. 2019;36(2):328–340. doi:10.1093/molbev/msy214

40. Lin Y, Zhang W, Li B, Wang G. Keratin 17 in psoriasis: current understanding and future perspectives. *Semin Cell Dev Biol*. 2022;128:112–119. doi:10.1016/j.semcdb.2021.06.018

41. Ni X, Lai Y. Keratinocyte: a trigger or an executor of psoriasis? *J Leukocyte Biol*. 2020;108(2):485–491. doi:10.1002/JLB.5MR0120-439R

42. Benhadou F, Mintoff D, Del Marmol V. Psoriasis: keratinocytes or Immune Cells - Which Is the Trigger? *Dermatology*. 2018;235(2):91–100. doi:10.1159/000495291

43. Zhou X, Chen Y, Cui L, Shi Y, Guo C. Advances in the pathogenesis of psoriasis: from keratinocyte perspective. *Cell Death Dis*. 2022;13(1):81. doi:10.1038/s41419-022-04523-3

44. Tollenaere MA, Hebsgaard J, Ewald DA, et al. Signalling of multiple interleukin (IL)-17 family cytokines via IL-17 receptor A drives psoriasis-related inflammatory pathways. *Br J Dermatol*. 2021;185(3):585–594. doi:10.1111/bjd.20090

45. Hawkes JE. Discovery of the IL-23/IL-17 Signaling Pathway and the Treatment of Psoriasis. *J Immunol*. 2018;201(6):1605–1613. doi:10.4049/jimmunol.1800013

46. Li H, Charruyer A, Weisenberger T, Khalifa A, Ghadially R, Ghadially R. 781 IL1α, IL6, and GMCSF are Downstream Mediators of IL17A that Promote Asymmetric Stem Cell Self-Renewal in Psoriasis. *J Invest Dermatol*. 2020;140(7):S103. doi:10.1016/j.jid.2020.03.795

47. Jiang M, Li B, Zhang J, Hu L, Dang E, Wang G. Vascular endothelial growth factor driving aberrant keratin expression pattern contributes to the pathogenesis of psoriasis. *Exp Cell Res*. 2017;360(2):310–319. doi:10.1016/j.yexcr.2017.09.021

48. Yan BX, Zheng YX, Li W, Chen JQ, Man XY. Comparative expression of PEDF and VEGF in human epidermal keratinocytes and dermal fibroblasts: from normal skin to psoriasis. *Discov Med*. 2018;25(136):47.

49. Schn MP, Manzke V, Erpenbeck L. Animal models of psoriasis—highlights and drawbacks. *J Allergy Clin Immun*. 2020;147(2):439–455. doi:10.1016/j.jaci.2020.04.034

50. A A, B B, M S, et al. Impact of Psoriatic Disease on Quality of Life: interim Results of a Global Survey. *Dermatol Ther (Heidelb)*. 2022;12 (4):1055–1064. doi:10.1007/s13555-022-00695-0

51. S E, C A, G I, et al. Systemic pharmacological treatments for chronic plaque psoriasis: a network meta-analysis. *Cochrane Database Sys Rev*. 2022;5:D11535.

52. van Winden MEC, van der Schoot LS, van de L'Isle Arias M, et al. Effectiveness and Safety of Systemic Therapy for Psoriasis in Older Adults: a Systematic Review. *JAMA Dermatol*. 2020;156(11):1229–1239. doi:10.1001/jamadermatol.2020.2311